

# Project GRAND's Search for Sub-TeV Gamma Rays Coincident with Swift Gamma Ray Bursts

Taiyo Wilson

2010 NSF/REU Program  
Physics Department, University of Notre Dame

Advisor:  
Professor John Poirier

## Abstract

Project GRAND is a cosmic ray experiment located north of the University of Notre Dame campus. The detector array measures  $100\text{ m} \times 100\text{ m}$  and consists of 64 huts of proportional wire chambers used to detect charged secondaries. When high energy gamma rays strike the atmosphere, muon secondaries detectable by GRAND are produced. These muons act as signatures for gamma ray primaries and were used to find potential angular and temporal coincidences with gamma ray bursts (GRBs) detected by NASA's Swift satellite. A list of eight GRBs was arranged by likelihood of detection by GRAND. It was first determined which GRBs were in the visible sky for GRAND. Additional criteria for probable detection include a low zenith angle and high muon flux at GRAND (estimated from Swift data). For each GRB, GRAND's data during the T90 time interval and within roughly  $\pm 2.7^\circ$  of the GRB's direction were used. From this data, the deviation of the muon flux from the background rate was determined.

## Project GRAND

Project GRAND (Gamma Ray Astrophysics at Notre Dame) is a cosmic ray detector experiment located north of the University of Notre Dame campus at  $86^\circ 13' \text{ W}$ ,  $41^\circ 04' \text{ N}$  and 222 m elevation above sea level. GRAND studies cosmic rays in two energy bands: a lower energy band of range 30 - 300 GeV for detecting single muons and a higher energy band of range 100 - 100,000 TeV for detecting cosmic ray showers. The field measures  $100\text{ m} \times 100\text{ m}$  and contains 64 huts laid out in an  $8 \times 8$  grid. Each hut houses a detector system comprised of eight planes (four pairs) of proportional wire chambers (PWCs) [1].

Each PWC plane consists of a grid of 80 parallel wires which are held to a potential of 2600 V from the grounded metal casing. The chambers are filled with a mixture of 80% argon and 20% carbon dioxide gas which leaves a trail of ions and electrons if disturbed by an ionizing particle. The potential difference causes these ions to be accelerated toward the nearest wire, disturbing additional gas molecules and creating more ions in the process; this is called gas amplification. As a result, a small pulse of current is formed on the wires

nearest the ionizing particle's path, allowing the particle's position to be tracked.

Each pair of PWCs tracks a particle's two-dimensional location with an  $x$ -plane (eastward) and a  $y$ -plane (northward). Denoting the  $z$ -direction as vertical, the top three pairs of PWCs project the particle's path into the  $xz$  and  $yz$  planes with a precision of  $0.3^\circ$  [2]. The fourth PWC pair is separated from the top three by a 50 mm thick steel absorber plate used for particle discrimination of muons from electrons. On a basic level, muons can be thought of as heavier electrons due to their similar interactions. Because of their greater mass ( $105.7\text{ MeV}/c^2$ ) muons are accelerated less through electromagnetic fields and do not emit as much bremsstrahlung radiation. This allows muons to penetrate through the 50 mm steel plate to the final PWC plane while the electrons are absorbed. Thus, GRAND recognizes a muon as aligned hits in all four PWC pairs, a method which is 96% accurate. Each PWC plane has an area of  $1.29\text{ m}^2$ , yielding an effective area of  $83\text{ m}^2$  for all 64 huts. GRAND's ability to identify particles and track their direction with high angular resolution make it ideal for tracking high energy cosmic rays.

## Gamma Ray Bursts

Gamma ray bursts (GRBs) are quick emissions, ranging from milliseconds to several minutes, of gamma rays associated with highly energetic explosions occurring in distant galaxies. These events are the most luminous electromagnetic events observed in the universe. Following the initial burst is a lower energy afterglow emitted at longer wavelengths, allowing the distance to the GRB to be known from the redshift of the light. The distance to GRBs is typically several billion light years. For these gamma rays to reach the Earth from this distance, they must be extremely energetic. (The energy released during a GRB is comparable to the amount the Sun will release in its 10 billion year lifetime.)

GRBs are categorized based on their duration. Long GRBs, those with duration greater than 2 s, are thought to be caused by the core collapse of massive, rapidly spinning, low-metallicity stars. These long GRBs are much more energetic, and thus easier to detect than short GRBs. When massive stars fuse their core to iron, they can no longer produce energy through nuclear fusion and collapse. This release of gravitational potential energy heats and expels the star's outer layers. If the star is spinning rapidly enough, the collapsing matter will cause the star to form a dense accretion disk which forces energy outwards at the rotational axis, due to a lower density, at relativistic speeds (0.99995c). These narrowness and direction of these jets or beams (2 - 20° from the rotational axis) explain the high intensity of the radiation and low detection rate on Earth.

If these relativistic jets are directed toward the Earth, the angular resolution of the direction of the GRB event is excellent. This is because cosmic gamma rays, unlike charged hadrons, are not deflected by the Earth's and

galactic magnetic fields. When cosmic gamma rays strike the Earth's atmosphere, they produce secondary pions which decay into muons which are subsequently detected by GRAND. These charged secondaries do undergo some deflection. Figures 1 - 3 and Table 1 show data taken from a FLUKA Monte Carlo simulation used to predict the properties of muons from cosmic ray primaries [3],[4]. Figure 1 shows the result of folding the multiplicity of muons at sea level ( $N_\mu/N_\gamma$ ) with the differential spectral index ( $d\Phi_\mu/dE_\gamma$ ) and half-maximum-height ( $\delta\theta_{xz}$ ) as a function of the primary gamma energy (dashed line with diamond points). The maximum of this plot at ~10 GeV means that of muons that reach the ground, the median energy of their gamma primaries is ~10 GeV. Figures 2 and 3 show that most muons with 10 GeV gamma primaries are produced at ~17 km above sea level and have an average energy ~4 GeV. A height of 17 km corresponds to 0.87 atm or 1131 g/cm<sup>2</sup>. The mean square deflection for a multiple scattered muon where  $v \approx c$  through the atmosphere is given by the equation [5]

$$\langle \theta^2 \rangle = 0.157 \frac{Z(Z+1)z^2 t}{A(pv)^2} \ln[1.13 \cdot 10^4 Z^{4/3} z^2 A^{-1} t]$$

$$\langle \theta^2 \rangle = 0.157 \frac{7(7+1)(1)^2 1131}{14(4000)^2} \ln[1.13 \cdot 10^4 7^{4/3} 1^2 14^{-1} 1131]$$

$$\theta = 1.54^\circ$$

where  $Z$  is the atomic number of nitrogen,  $z$  is the charge of a muon,  $t$  is the atmospheric pressure in g/cm<sup>2</sup>,  $A$  is the atomic weight of nitrogen, and  $pv$  is the energy of a muon in MeV.

The deflection of muons due to the Earth's magnetic field is given by the small angle approximation

$$\theta \approx \frac{l}{r} \quad r = \frac{pv}{qvB}$$

$$r = 4 \cdot 10^9 / (3 \cdot 10^8)(0.186 \cdot 10^{-4}) = 7.17 \cdot 10^5$$

$$\theta \approx 17 \cdot 10^3 / 7.17 \cdot 10^5 = 1.36^\circ$$

where  $l$  is the length of the magnetic field traversed by the muon,  $r$  is the radius of curvature of the muon's path,  $pv$  is an approximation of the muon's energy due to its ultrarelativistic speed in eV,  $q$  is the charge of the muon,  $v$  the velocity of the muon, and  $B$  is the strength of the Earth's magnetic field in tesla at GRAND's location.

The deflection of the muon from the initial path of the pion due to pion decay can be calculated as the inverse tangent of the muons resultant transverse momentum divided by its forward momentum. This model assumes a maximum muon deflection angle perpendicular to the original direction of the pion [6].

$$\theta = \tan^{-1}(p_t/p_f)$$

$$p_t = \frac{1}{2M_\pi} [(M_\pi + M_\mu + M_\nu)(M_\pi - M_\mu - M_\nu) \cdot (M_\pi + M_\mu - M_\nu)(M_\pi - M_\mu + M_\nu)]$$

$$p_f = \frac{1}{2(139.6)} [2(139.6 + 105.7) \cdot 2(139.6 - 105.7)]$$

$$p_f = 29.8 \text{ MeV}/c$$

$$\theta = \tan^{-1}(29.8/4000) = 0.43^\circ$$

where  $p_t$  is the momentum of the muon in the reference frame of the pion (transverse momentum),  $p_f$  is the momentum of the muon in the original direction of the pion, and  $M_\pi$ ,  $M_\mu$ , and  $M_\nu$  are the masses of pion, muon, and neutrino respectively. Figure 4 shows a two-body decay from the both the pion and stationary reference frames.

The deflection angles for each of the previous calculations are added in quadrature for a total muon angle error of  $2.01^\circ$ . This compares

favorably with the estimated  $d\theta$  value estimated by the FLUKA Monte Carlo simulation in Table 1 [7].

$$d\theta_{total} = \sqrt{\delta\theta_s^2 + \delta\theta_B^2 + \delta\theta_\pi^2}$$

$$d\theta_{total} = \sqrt{1.54^2 + 1.36^2 + 0.43^2}$$

$$d\theta_{total} = 2.01^\circ$$

## Swift Satellite

Swift is a NASA satellite launched in late 2004 designed to detect and analyze GRBs. With higher energy sensitivity and better angular resolution than previous satellites such as BATSE, and the ability to swiftly point its telescopes at new events, Swift has revolutionized the detection of GRBs and increased detection rate to around one GRB per day. Swift's Burst Alert Telescope (BAT) automatically detects GRBs and is able to point its X-Ray Telescope (XRT) and Ultra-Violet/Optical Telescope (UVOT) in the right direction within 50 - 70 s and 80 - 100 s respectively [8]. By using Swift's data of the spatial coordinates and photon flux of each GRB, the most likely events to be observed by GRAND can be determined.

In order observe GRAND's data in the direction of a GRB, the right ascension and declination taken by Swift must be converted into local altitude and azimuth values. Altitude and azimuth are defined as [9]

$$alt = \sin^{-1}[\sin(lat) \cdot \sin(dec) + \cos(dec) \cdot \cos(ha)]$$

$$az = \cos^{-1}[\frac{\sin(dec) - \sin(lat) \cdot \sin(alt)}{\cos(lat) \cdot \cos(alt)}]$$

and are solved using the following equations

$$ha = lst - ra$$

$$lst = [(6.6460556 + 2400.01512617 \cdot \frac{(jdate - 2415020)}{36525} + 1.0027379 \cdot UT - \frac{long}{15}] \bmod 24$$

where *lat* and *long* are GRAND's geographic coordinates, *ra* and *dec* are the right ascension and declination, *ha* is the hour angle, *lst* is the local sidereal time, *jdate* is the Julian date, and *UT* is the Universal Time.

The altitude and azimuth are converted into angles projected into the *xz* and *yz* planes. The tangents of these angles are

$$TX = \sin(az) / \tan(alt)$$

$$TY = \cos(az) / \tan(alt)$$

There are 80 cells in each PWC plane. GRAND interprets these projected angles as differences in cell number, *DX*, between the top and bottom PWCs. Figure 5 shows a diagram of how the projected angles are converted into *DX* with an error window of 2.7°.

### Data Analysis

Swift GRBs considered were detected from January 2005 - June 2010. Preliminary analysis was conducted to determine which GRBs would most likely be detectable by GRAND. First, the GRBs must have been within 62° of the local zenith to be detectable by GRAND. The GRBs were chosen based on an acceptance factor and estimated fluence at GRAND. The acceptance factor is

$$Acc = \cos^2(zen) \cdot [\cos(zen)(1 - TX / \tan(1.0821)) \cdot (1 - TY / \tan(1.0821))]$$

where the term in brackets represents the acceptance of the detector and the cosine squared term represents the muon's path

through the atmosphere. The estimated fluence at GRAND is

$$\Phi_G = \Phi_S \left(\frac{E_G}{E_S}\right)^{-\gamma} = \Phi_S \left(\frac{20}{.05}\right)^{-\gamma}$$

where  $\Phi_G$  and  $\Phi_S$  are the fluence at GRAND and Swift respectively,  $E_G$  and  $E_S$  are the energy levels detected by GRAND and Swift respectively, and  $\gamma$  is the photon index measured by Swift which expresses how the fluence of gamma rays falls off for higher energies. The product of *Acc* and  $\Phi_G$  is used to determine the final list of eight GRBs listed in Table 2.

The signal of each GRB is calculated as the difference between the total counts inside the T90 interval minus the background counts normalized to the time of the T90. The background rate is the average count rate over the time interval  $24 \times T90$  before and after the signal. The signal and signal error are calculated as

$$N_\mu = S - B_s$$

$$dN_\mu = \sqrt{\delta(S - B_s)^2 + \delta B^2}$$

where  $S$  is the total counts during T90,  $B_s$  is the background count during T90, and  $B$  is the average background rate. Assuming the muon count rate is a Gaussian distribution, the  $Z$ -value, or statistical significance, of each signal is calculated as

$$Z = \frac{N_\mu}{dN_\mu}$$

where the  $Z$ -value represents the number of standard deviations away from the mean. These results are summarized in Table 2.

## Conclusions

The results do not indicate any meaningful detection of excess muons coincident with gamma ray bursts. The number of positive and negative deviations in muon signal were even. The event with the highest statistical significance,  $1.73\sigma$ , was expected to be the least likely out of the eight GRBs considered. The  $Z$ -value of this event corresponds to a probability of  $4.2 \times 10^{-2}$ , which is not even statistically significant as a single event.

An improvement that was considered was altering the size of the angular window to see if this would yield a better signal. Figure 6 shows a peak signal  $Z$ -value at  $1.5\sigma$  angular width. Assuming our calculated angular uncertainty of  $2.07^\circ$  corresponds to  $1\sigma$ , the optimal angular window size would be  $3.11^\circ$ , which is not significantly greater than the  $2.7^\circ$  window size used.

Additional uncertainty exists in the way the photon index measured by Swift. Three of the indices were determined by using a power law with an exponential cutoff. Because Swift measures energies much lower, 50 - 150 keV, than what GRAND detects, the exponential cutoff makes the value for the estimated fluence at GRAND more uncertain.

## Acknowledgements

First, I would like to acknowledge my research advisor Dr. John Poirier for making my first real research experience enjoyable. His expertise, willingness to help, and congenial nature made for a very comfortable working environment where I could develop my research skills. I would also like to thank Dr. Christopher D'Andrea for providing guidance throughout the summer.

Finally, I would like to thank the University of Notre Dame and the National Science Foundation for giving me the opportunity to experience basic research. Dr. Umesh Garg, Shari Herman, and many others in the Notre Dame Physics Department for making the summer both educational and enjoyable.

- 
- [1] Project GRAND, <http://nd.edu/~grand/>.
  - [2] J. Poirier, C. D'Andrea et al (2007), Status report on project GRAND, *30th International Cosmic Ray Conference (ICRC)*.
  - [3] J. Poirier, S. Roesler, A. Fasso (2001), Distributions of secondary muons at sea level from cosmic gamma rays below 10 TeV, *Elsevier Science*.
  - [4] J. Poirier, S. Roesler, A. Fasso (2001), Calculation of atmospheric muons from cosmic gamma rays, *26th International Cosmic Ray Conference (ICRC)*.
  - [5] E. Segre, H. Staub et al (1953), Experimental Nuclear Physics Volume I, *John Wiley & Sons, Inc., New York*.
  - [6] P. Trower (1965), High Energy Particle Data Volume III: Kinematics of Particles as a Function of Momentum, *Lawrence Berkeley National Lab*.
  - [7] J. Poirier, S. Roesler, A. Fasso (2001), Muon angles at sea level from cosmic gamma rays below 10 TeV, *26th Cosmic Ray Conference (ICRC)*.
  - [8] Atteia, Jean-Luc, and Gilbert Vedrenne. "HETE-2 and Swift." *Gamma-Ray Bursts: The brightest explosions in the Universe* (Springer Praxis Books / Astronomy and Planetary Sciences). 1 ed. New York: Springer, 2009. 160. Print.
  - [9] A. Henden, R. Kaitchuck (1990), *Astronomical Photometry: Text and Handbook for the Advanced Amateur and Professional Astronomer*, *Willmann-Bell*.

[10] J. Poirier, C. D'Andrea (2003), Search for Sub-TeV Gamma Rays Coincident with BATSE Gamma Ray Bursts, *28th International Cosmic Ray Conference (ICRC)*.

## Appendix

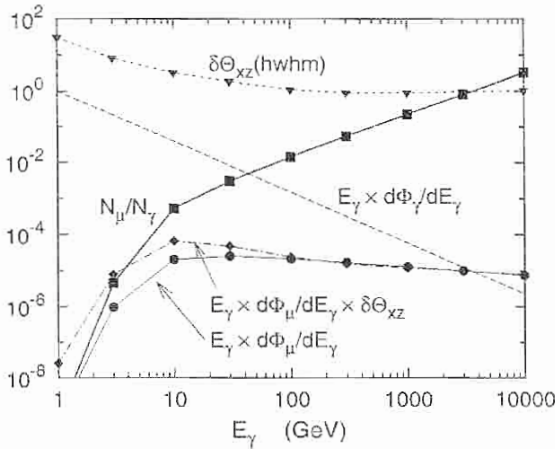


**Figure 1:** This graph shows the results of folding the the multiplicity of muons at sea level per primary gamma ( $N_\mu/N_\gamma$ ) with the energy spectrum of primary gamma rays ( $N_\mu/N_\gamma$ ) with the energy spectrum of primary gamma rays ( $d\Phi_\mu/dE_\gamma$ ) and the half-maximum-height ( $\delta\theta_{xz}$ ) as a function of the primary gamma energy (dashed line with diamond points).

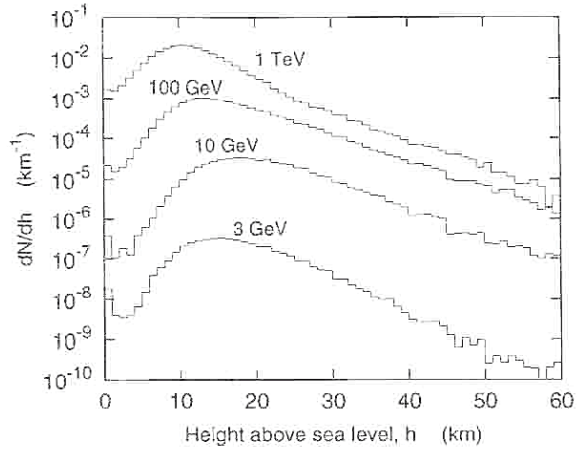


**Figure 2:** This graph shows the distribution of the production height of muons whose primary gammas have energy 3, 10, 100, and 1000 GeV.

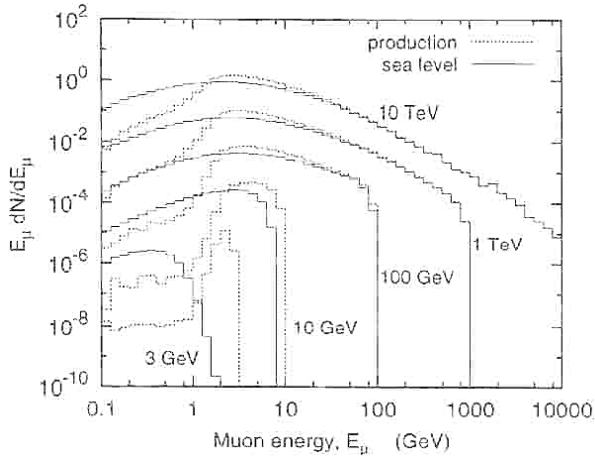


**Figure 3:** This graph shows the distribution of muon energy at their production height and at sea level for muons whose primary gammas have energy 3, 10, 100, and 1000 GeV.

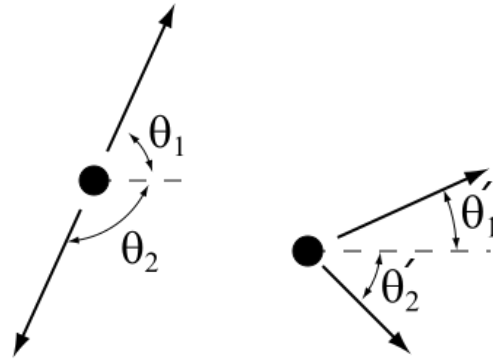


**Figure 4:** These diagrams show a two-body decay in the lab reference frame and in the reference frame of the incident particle, pion, decaying into a muon and muon neutrino.



## Appendix

	$E_{\gamma}$	$E_{\mu} > 0$		$E_{\mu} > 1$	$E_{\mu} > 2$	$E_{\mu} > 4$
		E-d.	E-d(b)	E-d.	E-d.	E-d.
n.f.	10	3.84	3.41	3.06	2.45	1.64
	1000	3.32	3.03	2.30	1.74	1.19
(1)	10	4.41	3.38	3.53	2.88	2.03
	1000	3.48	3.00	2.42	1.84	1.26
(2)	10	4.73	3.40	3.83	3.15	2.25
	1000	3.61	3.02	2.52	1.91	1.30
(3)	10	6.44	3.38	5.28	4.44	3.34
	1000	4.19	3.02	2.93	2.24	1.56

**Table 1:** This table shows the half-widths of the muon's sea level angular distribution due to varying magnetic field strengths, primary gamma energy, and secondary muon energy. Row (1) corresponds to the magnetic field strength for GRAND's geographic coordinates.

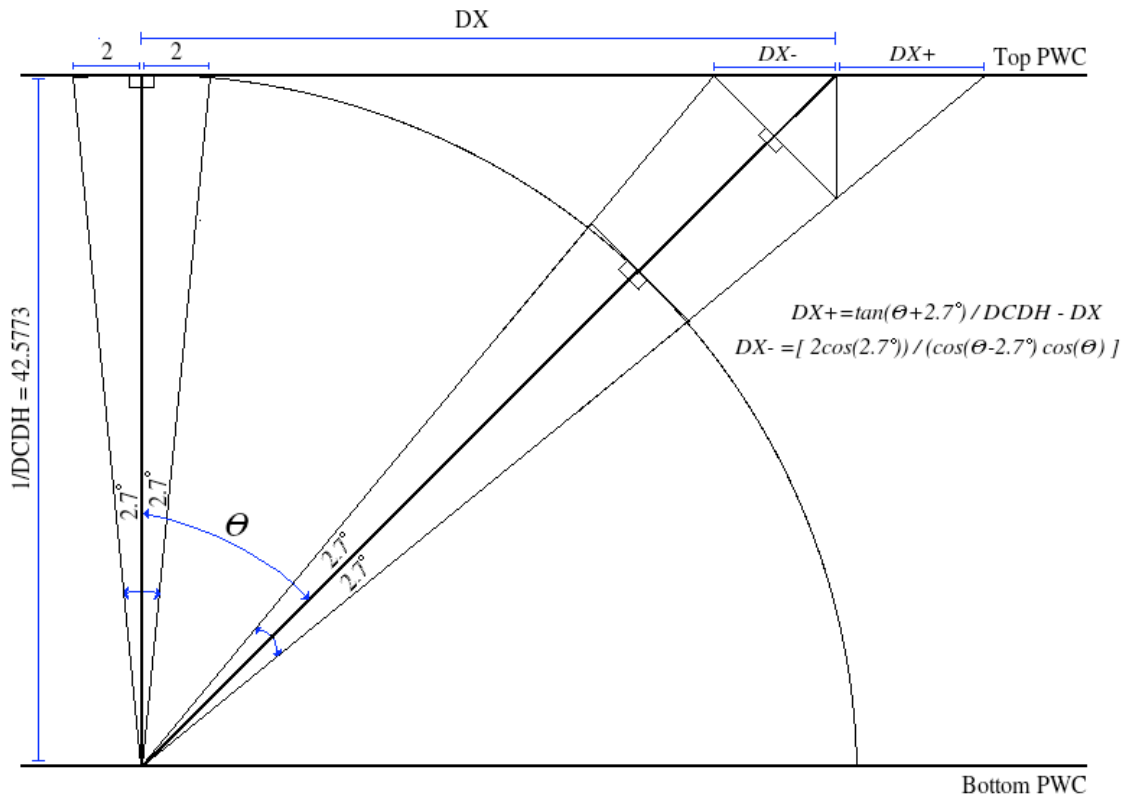


**Figure 5:** This diagram shows the projection of a muon path into the  $xz$  plane to be detected by GRAND's  $xz$  PWC planes. The angle of the muon ( $\theta$ ) is converted into a  $DX$  value which is the difference in cell number between the top and bottom planes (there are 80 cells). The angular window of  $\pm 2.7^\circ$  for a vertical angle varies with  $\theta$  and is also converted to a  $DX-$  and  $DX+$  value by the formulas above.

## Appendix

GRB	Time	T90	RA	Dec	Acc	$\Phi_G$	$100 \times \text{Acc} \times \Phi_G$	$N_\mu \pm dN_\mu$	Z
080319B	4396.3	45.124	14.5	36.3	0.6	1.59	91.23	$16.24 \pm 18.88$	$0.86\sigma$
060204B	34514	139.38	14.1	27.7	0.5	0.24	11.3	$6.54 \pm 12.15$	$0.538\sigma$
090618	12576	113.2	19.6	78.4	0.3	0.21	6.38	$-7.69 \pm 21.94$	$-0.351\sigma$
060428B	14112	96	15.7	62	0.6	0.07	4.11	$-15.06 \pm 25.80$	$-0.584\sigma$
061126	13710	70.84	5.77	64.2	0.6	0.02	1.44	$-17.5 \pm 22.42$	$-0.781\sigma$
081126	59660	55.8	21.6	48.7	0.8	0.02	1.22	$20.15 \pm 25.63$	$0.786\sigma$
06122A	80980	96	23.9	46.5	0.4	0.02	1.07	$-15.67 \pm 19.84$	$-1.055\sigma$
070616	41668	402.36	2.14	57	0.7	0.01	0.82	$100.53 \pm 58.24$	$1.73\sigma$

**Table 2:** This table is a summary of the eight GRBs analyzed. It lists the beginning of the T90 time, T90 duration, right ascension, declination, acceptance factor, estimated GRAND fluence, acceptance factor multiplied by fluence, signal and signal error, and the statistical significance or Z-value.

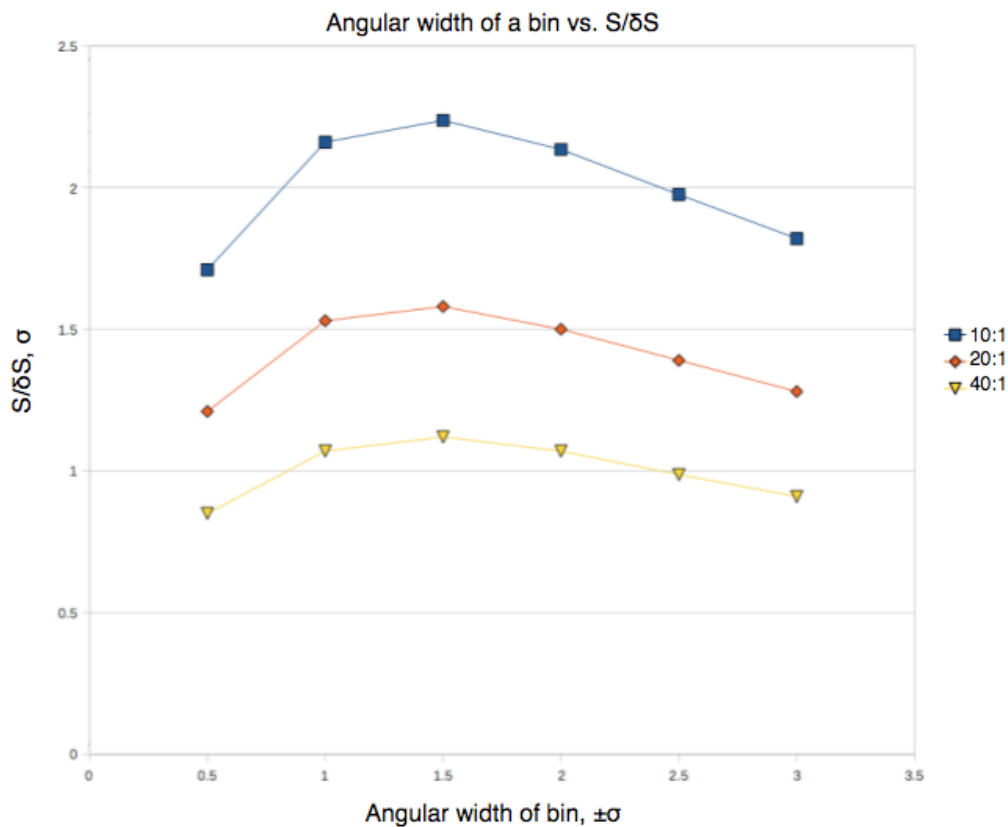


**Figure 6:** This graph shows the optimal angular window size for background to signal rates of 10:1, 20:1, and 40:1. The peak of this graph is  $\sim 1.5\sigma$ ,